Acute Striato-Cortical Synchronization Induces Focal Motor Seizures in Primates

Jerome Aupy, Bastien Ribot, Sandra Dovero, Nathalie Biendon, Tho-Hai Nguyen, Gregory Porras, Marc Deffains, Dominique Guehl, Pierre Burbaud

Acute Striato-Cortical Synchronization Induces Focal Motor Seizures in Primates

Jerome Aupy, Bastien Ribot, Sandra Dovero, Nathalie Biendon, Tho-Hai Nguyen, Gregory Porras, Marc Deffains, Dominique Guehl, Pierre Burbaud

OXFORD UNIVERSITY PRESS | Cerebral Cortex

Acute striato-cortical synchronization induces focal motor seizures in primates

Journal:	*Cerebral Cortex*
Manuscript ID	CerCor-2020-00186
Manuscript Type:	Original Article
Date Submitted by the Author:	03-Mar-2020
Keywords:	epilepsy, basal ganglia, seizure, network, interneurons

Complete List of Authors:
AUPY, Jerome; University of Bordeaux College of Health Sciences, Bordeaux Neurocampus, IMN, UMR CNRS 5293; Bordeaux University Hospital, CHU BORDEAUX
Ribot, Bastien; University of Bordeaux College of Health Sciences, Bordeaux Neurocampus, IMN, UMR CNRS 5293
dovero, sandra; University of Bordeaux College of Health Sciences, Bordeaux Neurocampus, IMN, UMR CNRS 5293
Biendon, Nathalie; University of Bordeaux College of Health Sciences, Bordeaux Neurocampus, IMN, UMR CNRS 5293
Nguyen, Tho-Hai; University of Bordeaux College of Health Sciences, Bordeaux Neurocampus, IMN, UMR CNRS 5293
Deffains, Marc; University of Bordeaux College of Health Sciences, Bordeaux Neurocampus, IMN, UMR CNRS 5293
Guehl, Dominique; University of Bordeaux College of Health Sciences, Bordeaux Neurocampus, IMN, UMR CNRS 5293
Burbaud, Pierre; University of Bordeaux College of Health Sciences, Bordeaux Neurocampus, IMN, UMR CNRS 5293

Note: The following files were submitted by the author for peer review, but cannot be converted to PDF. You must view these files (e.g. movies) online.

3-D_Rats.avi
3-D_primate.avi

Acute striato-cortical synchronization induces focal motor seizures in primates

Aupy J. MD PhD [1, 2] *, Ribot B. PhD [1] *, Dovero S. PhD [1], Biendon N.[1], Nguyen T-H. [1], Porras G., Deffains M. PhD [1], Guehl D. MD PhD [1, 2], Burbaud P. MD PhD [1, 2].

* These authors contributed equally to the study.

Author's affiliations

[1] University of Bordeaux, Bordeaux Neurocampus, IMN, UMR CNRS 5293, Bordeaux, France

[2] Bordeaux University Hospital, Department of Clinical Neurosciences, Bordeaux, France

Correspondence to

Jerome Aupy

Bordeaux University Hospital, Department of Clinical Neurosciences

Place Amelie Raba-Leon, 33076, Bordeaux, France

University of Bordeaux, Bordeaux Neurocampus, IMN, CNRS UMR 5293

146 Rue Leo Saignat, 33076 Bordeaux, France

Tel. +33556795513

Email: jerome.aupy@u-bordeaux.fr

Formatting

Abstract: 211

Manuscript: 4967

Figure: 4

Table: 1

Number of references: 50

Abstract

Objective: Whether the basal ganglia are involved in the cortical synchronization during focal seizures is still an open question. In the present study, we proposed to synchronize cortico-striatal activities acutely inducing striatal disinhibition, performing GABA-antagonist injections within the putamen in primates.

Method: Experiments were performed on three fascicularis monkeys. During each experimental session, low volumes of bicuculline (0.5 to 4 µL) were injected at a slow rate of 1 µL/min. Spontaneous behavioural changes were classified according to Racine's scale modified for primates. These induced motor behaviours were correlated with electromyographic (EMG), electroencephalographic (EEG) and putaminal and pallidal local field potentials (LFP) changes in activity.

Results: acute striatal desinhibition induced focal motor seizures. Seizures were closely linked to cortical epileptic activity synchronized with a striatal paroxysmal activity. These changes in striatal activity preceded the cortical epileptic activity and the induced myocloniae and both cortical and subcortical activities were coherently synchronized during generalized seizures.

Interpretation: Our results strongly suggest the role of the sensorimotor striatum in the regulation and synchronization of cortical excitability. These dramatic changes in the activity of this "gating" pathway might influence seizure susceptibility by modulating the threshold for the initiation of focal motor seizures.

Key words

Basal ganglia, striatum, epilepsy, seizures, interneurons

INTRODUCTION

Epilepsy has long been considered as a disease of cortical origin. However, recent evidence suggests that epileptic seizures involve a widespread interaction between the cortical and subcortical structures (Deransart and Depaulis 2002; Norden and Blumenfeld 2002; Paz and Huguenard 2015; Vuong and Devergnas 2017). Among the latter, the basal ganglia (BG) constitute a network of interconnected nuclei involved in sensorimotor, cognitive and emotional integration (DeLong and Wichmann 2010). Their input structures, the striatum and the subthalamic nucleus (STN), receive information from almost the whole cortex (Haber 2016). In turn, their output nuclei (internal globus pallidus (GPi) and substantia nigra pars reticulata (SNr)) are massively connected via inhibitory projections to the thalamo-cortical pathways (Bolam et al. 2000). Experimental studies in rodent models of generalized absence epilepsy have shown that the BG network may play a key role in the production, development and maintenance of seizures (Deransart et al. 1998; 2000; Slaght 2004; Paz et al. 2005; Arakaki et al. 2016). However, data obtained from animal models of focal epilepsies remain sparse (Neafsey et al. 1979; Kaniff et al. 1983; Dybdal and Gale 2000; Devergnas et al. 2012). Thus, whether the BG are involved in focal seizures, either passively by propagation or actively in the synchronization of cortical activity via the striato-thalamo-cortical pathway, is still an open question.

The striatal projections neurons (SPNs) are under the control of tonic GABAergic inhibition applied by parvalbumin-positive "fast-spiking" interneurons (Koos and Tepper 1999a), which may be involved in centre-surround-type inhibitory processing (Mallet et al. 2005). This hypothesis posits that they regulate the level of synchrony of SPNs (Gittis et al. 2010) and potentially that of the striato-thalamo-cortical pathway during seizures (Aupy et al. 2019). In addition, previous experiments have shown that microinjections of GABAergic antagonists in the sensorimotor striatum can induce choreic movements (Crossman et al. 1988) and myoclonic tics (MARSDEN et al. 1975; Crossman et al. 1988; TARSY et al. 2005; Darbin and Wichmann 2008; McCairn et al. 2009; Worbe et al. 2009; Gittis et al. 2011). These movement disorders presumably result from an increased cortical excitability due to a reduction in the GPi/SNr inhibitory inputs to the thalamus (McCairn et al. 2009). The latter might be caused either by decreased excitation from the subthalamic nucleus (STN) or by increased inhibition from the striatum (Albin et al. 1989; DeLong and Wichmann 2007). However, the possibility that epilepsy might be due to BG dysfunction has never been evoked. Motor focal seizures are usually characterized by transient motor behaviour that occurs simultaneously with hypersynchronous paroxystic cortical activity. Interestingly,

myoclonuses and hyperkinetic behaviours can be a semiologic features of focal seizures, especially those originating from the frontal lobe (Bonini et al. 2013).

Considering these previous data, we questioned the potential role of the sensorimotor striatum in the cortical synchronization during focal seizure and potentially in their genesis.. To this end, we performed microinjections of the GABAergic antagonist bicuculline into the sensorimotor striatum of non-human primates (NHP) in order to induce motor focal seizures. Thereafter, we correlated the induced motor behaviour with cortical and subcortical electrophysiological changes. We demonstrate that focal disinhibition of the sensorimotor striatum can induce focal motor seizures correlated with dramatic changes in electrophysiological activity within both the basal ganglia and the motor cortices.

METHOD

Animals

Experiments were performed on three fascicularis monkeys (*Macaca fascicularis)*, two males (Ze and Di) and one female (Ra) weighing between 5 and 7 kg. Care and treatment were in strict accordance with the National Institute of Health guidelines (2010/63/EU) and the European Community Council Directive for experimental procedures in animals (86/609/EEC) and the French National Committee (CE50/4612).

Surgical procedure

Surgical procedures were conducted under aseptic conditions under generalized anaesthesia (gaseous anaesthesia, isoflurane 1.5-2%, nitrous oxide 1% and oxygen) after induction with intramuscular ketamine HCl (10 mg/kg), atropine sulfate (0.5 mg/kg) and diazepam (0.5 mg/kg).

The site of injections was determined on presurgical MRI and compared to a stereotactic atlas. A 30-gauge stainless steel cannula guide (Plastic One Inc. ®) was inserted towards the sensorimotor striatum. The tip position was calculated to be 2 mm above the striatum, approximately 2.5 mm posterior to the anterior commissure and 12 mm lateral to the interhemispheric line, in accordance with the coordinates of the sensorimotor putamen (Worbe et al. 2009) and macaca fascicularis atlas (Szabo and Cowan 1984). The cannula guide was then fixed on the skull with titanium bone screws and methyl-methacrylate cement (Refobacin® Bone cement LV, Zimmer Biomet©). Stereotactic coordinates of the cannula guide tip are shown in supplemental data. In monkey 1, implantation was done under stereotactic conditions in relation to the anterior commissure (CA) and interhemispheric line using the macaca fascicularis stereotactic atlas (Szabo and Cowan 1984). In monkeys 2 and 3,

it was done under MRI-guided neuronavigation (Brainsight®, Rogue Research, Canada) and compared to stereotactic coordinates. This validated method allowed us to reach specific target areas accurately in the non-human primate brain including the striatum, GPi or cortical landmarks (Frey et al. 2004).

Cortical activity was recorded chronically using electroencephalographic wires (AS-634 Cooner Wires, USA) fixed in the skull using titanium bone screws and methyl-methacrylate cement. Electrode positions were determined on presurgical MRI and compared to the stereotactic atlas. The following regions were targeted: bilateral primary motor cortex (forelimbs and hind limbs) and supplementary motor area. Reference and mass were placed on the parieto-occipital cortex contralaterally to the site of injection.

Lenticular nucleus (including the putamen, the GPe and the GPi) activity was recorded chronically using a linear microelectrode array implanted within the striatum and the pallidum, in its external and internal segments, ipsilateral to the injection site. The position of the linear microelectrode arrays (LMA, Alpha Omega, Israel; impedance: 0.5-1 MOhms at 1KHz, wire diameter: 25µm) was determined on presurgical MRI, then compared to the stereotactic atlas. The LMA tip targeted the mesial part of the GPi and was inserted at a 45° angle to the axis passing through the interhemispheric line in the coronal plane (see supplemental data for stereotactic coordinates of the GPi tip). The LMA was fixed in the skull using titanium bone screws and methyl-methacrylate cement. Electrode length was 11.2 mm to allow the simultaneous recording of the whole lenticular complex. Reference and mass were inserted under the subdural space.

Microinjections

During each experimental session, the animal was placed in a standard primate chair enabling head movement to be partially restrained. A 27-gauge injection cannula (Plastic One Inc. ®) connected via a Delrin manifold to a 10-ml syringe (Hamilton, Reno, NV, USA) was inserted into the sensorimotor striatum (extending 2.5 to 4 mm beyond the cannula guide tip) and left in place throughout the experiment. We used sterile bicuculline methiodide (Tocris Bioscience, United Kingdom), a potent antagonist of GABA-A receptor channels, dissolved in physiological saline at a concentration of 15 µg/µL (29.5 mmol/L). Low volumes of bicuculline (0.5 to 4 µL) were injected slowly at 1 µL/min. Different control sessions with saline (NaCl 0.9%) microinjections were administered with the same protocol and volumes.

At the end of the experimental sessions and before overdosing of anaesthetic drugs, we performed injections of cholera-toxin B (CTB), contralaterally to the site of drug injection in order to estimate the volume of drug diffusion. We used the same methodology as previously

described, injecting CTB in the sensorimotor striatum at a low volume (2 µL in rats and 4 µL in primate) and slow rate of 1 µL/min.

Behavioural Analysis

Spontaneous behaviours were recorded during each experimental session using a high-definition multi-channel video system (Ipela SNC, Sony©). Digital videos were stored on a hard drive for offline analysis. Video sessions lasted at least 45 min and were extended if necessary. As soon as it became obvious that drug injections induced abnormal involuntary movements, we used a modified version of Racine's scale previously used in a kindling model of rodent seizures (Racine 1972). The scale has also been used in primates (Bachiega et al. 2008; Perez-Mendes et al. 2011). Thus, video sessions were retrospectively and blindly scored every 30s by a neurologist specialized in epilepsy (JA). Our modified Racine's scale (mRS) was classified as follows:

I. Abnormal orofacial automatisms, including hypersalivation, "mouth-cleaning-like" behaviour and tongue automatisms

II. Clonus restricted to one anatomical localization either orofacial or forelimb

III. Clonus involving two different anatomical localizations including orofacial and forelimbs

IV. Clonus involving three anatomical localizations including orofacial, forelimbs and hind limbs or axial body parts (including straub tail or arched body posture)

V. Bilateralisation or tonic-clonic generalization with or without postural impairment

Electrophysiological recordings

During each session, we recorded simultaneously electromyographic (EMG), electroencephalographic (EEG) and intracerebral local field potential (LFP) activities. *EMG recordings:* EMG activity was recorded using a trignoTM Wireless system (Delsys inc., USA). Sensor stickers (TrignoTM Flex Sensor) were used to record the extensor and flexor carpi radialis activity contralateral to the injection site. EMG signals were sampled at 1KHz and sent wirelessly to the receiving computer. *EEG recordings:* Bipolar EEG recordings were performed using the multichannel system. EEG signals were sampled at 10KHz. *LFP recordings:* LFPs from the sensorimotor putamen, the GPe and GPi were recorded through 24 contacts of platinum-iridium linear microelectrode arrays. Intracerebral lenticular nucleus signals were sampled at 20KHz. Neuronavigation and histopathology data allowed us to reconstruct the electrode position within the lenticular complex on the presurgical MRI. Thus, contacts were classified as follows: putamen contacts, GPe contacts and GPi contacts. The contacts located at the edge of each structure were not taken into consideration in the analysis

to avoid any anatomical localization error. Both EEG and LMA were connected to a 32-channel connector (Omnetics, USA) and sent wirelessly to the receiving computer (advanced wireless W2100, MultiChannel System©, Germany). Supplemental data figure 1 summarizes the injection and recording method.

Electrophysiological Analysis

Firstly, EMG, EEG, LFP signals were synchronized together as well as with the video recordings, stored and processed offline using Matlab 2017a (Mathworks, Natick, MA, USA). EEG and LFP signals were analysed using a bipolar montage (between two adjacent contacts) and band-pass filtered between 0.5 and 300Hz. They were normalized for each experimental session and the EMG signal was rectified (normalized and rectified signal $= \left|\frac{u^n - \bar{u}}{StD_u}\right|$, with u the signal value over time, $\bar{u}$ the average signal over the experimental session and StD_u its standard deviation).

Definition of regions of interest (ROIs): We analysed the correlation between signals locally recorded from different regions of interest (ROIs) chosen and standardized as follows:

a. As the paroxystic activity was seen mainly on the electrodes recording the primary motor cortex, we analysed the electroencephalographic bipolar signal recorded from the forelimb primary motor cortex.

b. Dorsolateral striatum (Putamen)

c. Globus pallidum externus (GPe)

d. Globus pallidum internus (GPi)

Definition of period of interest (POIs): To quantify the interaction during seizure activity between the cortex and the subcortical regions explored and to compare them with background, three periods of interest (POIs) were chosen:

a. Background activity (BKG): several background periods without artefacts (at least 50 per monkey, all lasting 10s) were chosen randomly during NaCl control injections and used as reference periods.

b. Myoclonic jerks: including periods of 10 artefact-free seconds corresponding to focal myoclonic activity interpreted as motor seizures (mRS = II or III)

c. Generalized tonic-clonic movements: including the first 10 seconds after the beginning of generalized abnormal movement interpreted as tonic-clonic seizures (mRS = IV or V).

EEG analysis: To compare the number of spikes during each POI, an automatic spike-and-wave detection was applied on the EEG forelimb primary motor derivations (sampling 1 KHz, bipolar montage, band-pass filtered between 0.5 and 300Hz) on each POI. This consisted in calculating a mean spike discrimination level during the generalized tonic-clonic movement period. This was later applied on the other POIs. A standard deviation of 2.0 clearly allowed the spikes to be discriminated from the baseline signal. Spike numbers for each POI were then compared using a one-way ANOVA and unpaired Student's t-test after Bonferroni correction for multiple comparisons (IBM SPSS statistics 22®). A P-value < 0.05 was considered significant.

In addition, to analyse the temporo-spectral content of EEG signals during generalized tonic-clonic movements, we performed a time frequency analysis (TFA). TFA assesses the changes in the involved region with a good resolution in both time and frequency. (TFA – bipolar montage following the application of a bandpass filter of 1 to 200 Hz. Complex Morlet wavelet analysis was performed in Matlab using a central frequency of 1Hz and a temporal resolution (Full Width Half Maximum) of 6s).

Back-averaging analysis: EMG, EEG and LFP activities were inspected visually and muscular jerk onsets (characterized by a brief and dramatic increase in muscular activity, both on video and EMG signals) were tagged. To compare the latencies between the myoclonic activity and EEG or LFP, a back-averaging analysis was performed. The objective was to average EEG and LFP signals preceding the onset of myoclonia in order to detect the existence of a pre-myoclonic potential related to muscular activity. The latencies were calculated using a first derivative function on the signal thus obtained. A standard deviation of 2.5 was considered significant. Latencies were then compared between ROIs using a two-way ANOVA and paired Student t-tests after Bonferroni correction for multiple comparisons (IBM SPSS statistics 22®). A P-value < 0.05 was considered as significant.

Coherence analysis: As we wanted to determine whether neuronal oscillations at similar frequencies between the cortex and basal ganglia were engaged in functional coupling during seizures, we performed magnitude-squared coherence analysis. Coherence was estimated for 1-second sliding windows of EEG and LFP signals, overlapping by 500 ms, for each POI and each ROI, and averaged for each experimental session. Frequency bands were

defined as follows: delta [0.5 – 3] Hz; theta]3 – 8] Hz; alpha]8 - 12] Hz; beta]12 – 25] Hz; gamma]25 - 70]. To compare coherence, mean values of the coherence between each ROI in each frequency band were compared using a two-way ANOVA and paired Student t-tests after Bonferroni correction for multiple comparisons. A P-value < 0.05 was considered as significant.

Histology

At the end of the experimental sessions, animals received an overdose of anaesthetic drugs (pentobarbital 50 mg/kg) and were transcardially perfused with 0.9% physiological saline solution. For the monkey, the brain was removed. The two hemispheres were divided and cut in three parts each. These tissues were post-fixed in a large volume of 4% buffered paraformaldehyde solution for one week at 4°C and cryoprotected in successive baths of 20% and 30% sucrose solution diluted in 0.1M phosphate-buffered saline (PBS) at 4°C until they sunk. For the rats, brains were removed and post-fixed for 5 days and cryoprotected in 20% sucrose-PBS only. Finally, brains were frozen by immersion in an isopentane bath at -55°C for 5 minutes and stored at -80°C. The entire striatum was cut in the coronal plane on a Leica 3050S cryostat into 50-µm serial free-floating sections (12 series for rat and 24 series for monkey) collected in PBS-azide 0.2% and stored at 4°c.

To estimate the extent of drug diffusion, we performed immunostaining raised against CTB on serial striatal sections of two rat brains and one monkey brain (monkey 3). Briefly, sections of one series for each were blocked in a solution of BSA 2%-TritonX100®0.3%-PBS 0.1M for 30 minutes before incubation overnight in a goat polyclonal anti-CTB antibody (#227040, Merck, France) diluted at 1:20.000 in BSA 0.2%- TritonX100®0.3%-PBS 0.1M. After rinsing sections through PBS, the stain was revealed by 30-min incubation in an HRP-anti-goat polymer system (goat ImmPRESS Kit VECTOR, France), followed by DAB revelation for a few seconds (DAKO DAB Kit, #K346811-2, Agilent, France). Free-floating sections were mounted on slides, counterstained with 0.2% cresyl-violet solution, dehydrated and coverslipped. Then, high-resolution whole slide images were acquired with a Panoramic SCAN (3D Histech, Hungary) at x20 magnification. The volume of the striatum and CTB staining area were estimated with Cavalieri's formula using Mercator software (Mercator V7.13.4, Explora Nova, France). In addition, the high-resolution pictures obtained were also used to visualize the microinjection sites based on the traces due to the passage of the cannula and electrodes.

RESULTS

Injections

A total of 39 bicuculline injections were administered in three monkeys (Table 1). Histological reconstruction confirmed that neuronavigation and stereotactic implantations targeted the sensorimotor part of the putamen, posterior to the anterior commissure (Figure 1A). The electrode targeted the tip of the GPi with a 45° angle and crossed the entire lenticular nucleus (GPi, GPe and Putamen, Figure 1B). Additional immunohistological studies in two rats and one monkey showed that the CTB did not diffuse to more than 17.8 % of the entire putamen volume (supplemental data) and remained confined within it, without any cortical diffusion (Figure 1C and 1D).

Behavioural effects

Of the 39 bicuculline injections, 29 (74.3%) produced dramatic behavioural changes. Figure 2A represents the average mRS during bicuculline injections for each monkey compared to NaCl injections. These effects were reproducible and observed in the three animals studied. They were characterized by myoclonic jerks contralateral to the site of injection, clearly different from the monkeys' normal behaviour and easily detectable on video. Myoclonia could affect different muscle groups, including the orofacial musculature, the neck musculature, the proximal or the distal part of the forelimbs, the proximal part of the hind limbs, the axial musculature and the tail. Once started, the myoclonia abated only when diazepam (1mg/Kg, Valium®, Roche, 10mg/2ml) was injected i.m. In monkey 1, myoclonic activity started on average 23.3 ± 14.6 min after the beginning of the injection with orofacial involvement (activation of the zygomaticus major muscle, associated with ipsilateral and abnormal blinking corresponding to eyelid myoclonia). Progressively, the myoclonia tended to become rhythmic and affected other muscular groups with a "Jacksonian march" starting with the ipsilateral proximal forelimb (activation of the deltoid and biceps brachialis), sometimes followed by the ipsilateral proximal hind limbs (activation of the ilio-psoas). In monkeys 2 and 3, myoclonia started on average 19.9 ± 19.4 min and 5.3 ± 4.3 min after the beginning of the injection, respectively. It initially involved the distal segment of the forelimbs (activation of the fingers and wrist extensors), later evolving with a "Jacksonian march", with involvement of the proximal forelimbs and orofacial musculature, sometimes followed by myoclonic jerks of the proximal hind limbs. Interestingly, the three monkeys also presented generalized tonic-clonic seizures (GTC, 20.5% of the injections). On the other hand, NaCl sham injection of the same volume never produced any myoclonia or abnormal

behaviour. Figure 2B shows an example of the temporal evolution of behavioural changes during bicuculline injections for each monkey and average mRS for each monkey and conditions.

Visual inspection and anatomic-electrophysiological correlations

EMG analysis: Myoclonic jerks were clearly detectable on the EMG signal as short stereotypical EMG bursts contralateral to the injection site. Quantification of the myoclonic events was derived from the rectified and filtered EMG signal. As the recording session progressed, these myoclonic short EMG bursts could be directly followed by a longer and more tonic activity that was concordant with the behaviour recorded with the longer abnormal tonic posturing immediately following the myoclonic jerk. GTC seizures were characterized by a disorganized, complex, EMG activity associating myoclonic EMG bursts superimposed on a permanent EMG tonic activity that lasted throughout the GTC (Figure 3A).

EEG analysis: Visual analysis of EEG recordings revealed abnormal paroxysmal activity characterized by spikes and spike-and-waves. Their maximum amplitude was seen on the electrodes located above the primary motor cortex ipsilateral to the site of injection and with a lesser amplitude over electrodes located above the SMA. Myoclonia was always concomitant with spike-and-waves, even though not all spike-and-waves could have triggered this specific behavioural manifestation. During GTC seizures, a progressive increase in frequency and amplitude of spike-and-wave activity was observed (Figure 3B). During GTC, this activity diffused to other derivations including SMA, then to the contralateral primary motor cortex (supplemental data). The end of seizure was characterized by an abrupt offset followed by the diffuse flattening of EEG activity (supplemental data). These results were confirmed by the time frequency analysis (figure 3C). In addition, the automatic spike-and-wave detection showed a clear increase in the number of spikes-and-waves between GTC seizures and sham injections (mRS = 4 or 5, $p < 0.0001$, Student's t-test), myoclonic activity and sham injections (mRS = 2 or 3, $p < 0.0001$) and between GTC seizures and myoclonic injection (mRS = 0, $p < 0.0001$) (Figure 4A).

LFP analysis: Concomitant to the EEG spikes-and-waves and myoclonic jerks, paroxysmal activity was also recorded at the subcortical level within the striatum, GPe and GPi. Figure 3D shows an example of ictal LFP activity.

Back-averaging analysis: To compare the latencies between the occurrence of EMG myoclonic activity and EEG and LFP, a back-averaging analysis was performed. On average, electrophysiological modification appeared -28.5 ± 8.6 ms before the onset of myoclonus in

the putamen; -29 ± 11.5 ms in the GPe; -23.8 ± 8.6 ms in the GPi and -15.9 ± 12 ms in the primary motor cortex. Therefore, changes in striatal activity appeared before changes in cortical activity ($p = 0.016$ and $p = 0.0015$, Student t-test, respectively for monkeys 1 and 2); changes in GPe activity appeared before changes in cortical activity ($p = 0.019$ and $p = 0.0105$ respectively for monkeys 1 and 2); and changes in GPi activity began before cortical activity in monkey 2 only ($p = 0.018$). Figure 4B provides the averaged results of back-averaging analysis. Figure 4C shows the average results of the back-averaging latencies for each structure and each monkey. In addition, one seizure was recorded only at the subcortical level.

Cortico-subcortical functional coupling during seizures: In comparison with background activity (after saline injections), during GTC seizures (mRS = 4 – 5) there was a significant increase in cortex-putamen, cortex-GPe and cortex-GPi magnitude-squared coherence within all the frequency bands ($p < 0.0001$, Student t-test) (Figure 4D).

DISCUSSION

We demonstrate for the first time that local pharmacological manipulations of the sensorimotor striatum in non-human primates induce abnormal movements similar to the focal motor seizures seen in humans, with or without generalization.

Previous studies using a similar injection protocol found that the drug diffused locally up to 1 mm from the Microdialysis probe (Westerink and De Vries 2001). Yoshida et al. demonstrated that bicuculline injected using the same parameter spreads as an ellipsoid of an approximate radius of 1.5 mm around the injection site (Yoshida et al. 1991). More recently, Worbe et al. investigated the local modification of neuronal activity induced by bicuculline to determine the speed of drug diffusion around the injection site. They found that during higher volume injections (3µL), neuron modifications could be recorded up to a distance of 1000 µm from the injection site (Worbe et al. 2009). In addition, the results of our immunohistological studies performed in rats and non-human primates showed that the volume of diffusion of CTB was lower than 18% of the entire putamen volume and remained confined within the latter, without cortical diffusion. Thus, it is very unlikely that the pharmacological effect of the bicuculline occurred outside the striatum surrounding the injection cannula.

Bicuculline is a well-known GABA-A inhibitor that can induce disinhibition of the neurons surrounding the injection site. The abnormal movements we observed after intra-striatal bicuculline injections are very similar to those observed in human focal motor seizures

with or without tonic-clonic generalizations. These manifestations were due to a specific effect of the drug, as NaCl sham injections never produced any particular behavioural changes. The apparent variability in the time to onset of the first abnormal movement could be related both to the effective volume of the drug injected and to the location of the injection site regarding the sensorimotor part of the putamen (as shown by Worbe et al. (Worbe et al. 2009)).

The main effect of GABAergic antagonists was contralateral myoclonia, which involved the orofacial regions and/or the upper limb, spreading to the lower limb and then contralaterally, as in human secondary tonic-clonic generalizations. This kind of "Jacksonian march" is concordant with the available striatal somatotopic data in monkeys (Miyachi et al. 2006; Nambu 2011). The cannula tips are located within the medial part of the sensorimotor striatum, which usually corresponds to the limit between the upper limb and facial territories. If the initial ventral diffusion of bicuculline is due to the way the drug is injected, it is logical that the facial or upper limb territories were the first involved by the injected drug.

Abnormal movements (either myoclonia or generalized tonic-clonic seizures) were well correlated to cortical EEG spikes-and-wave activity, which is pathognomonic of epilepsy. Spike-and-wave discharges result from the abnormal synchronization of a large population of cortical pyramidal cells and are considered as the EEG hallmark of epileptic activity (Wong et al. 1984). In addition, the localization of this paroxysmal activity over the primary motor cortex is concordant with the topography of myocloniae. Likewise, generalized tonic-clonic seizures occurred with the spreading of the EEG discharges over the different recorded regions and were associated with an increase in frequency and amplitude of the spike-and-wave rhythmic activity. This confirms that the bicuculline-induced abnormal movements were epileptic.

Similar behavioural manifestations have been previously reported after striatal GABAergic antagonist injections with a similar protocol (MARSDEN et al. 1975; Crossman et al. 1988; TARSY et al. 2005; Darbin and Wichmann 2008; McCairn et al. 2009; Worbe et al. 2009; Gittis et al. 2011) and were defined as myoclonus, chorea, tetanic episodes or tics. Nevertheless, the possibility that these abnormal movements may be of epileptic origin has never been envisaged.

Our data demonstrate that the first electrophysiological activity (LFPs) changes were recorded within the striatum and the pallidum before spreading to the motor and premotor cortices. LFPs are classically considered as the sum of the post-synaptic activity of a limited population of neurons located around the recording electrode (Mitzdorf 1985; Buzsáki et al.

2012). Consequently, the paroxysmal activity of LFPs corresponds to the synchronized activity of the neural population around the recording site, i.e. the striatum, GPe, GPi and then the primary motor cortex. The use of a bipolar configuration for the recordings with a short distance between two adjacent contacts makes the possibility that a distant field (cortical) contributed to the basal ganglia activity very unlikely (Lalla et al. 2017; Marmor et al. 2017). Moreover, the existence of multiple phase inversions (supplemental data) between contiguous bipolar contacts closely reflects the locally generated subcortical activity.

Back-averaging analysis over hundreds of myoclonic episodes demonstrated that the first evoked potential appeared within the striatum before the primary motor cortex and before the occurrence of the myoclonic jerks. Moreover, and decisively, one seizure was recorded only at the subcortical level without any obvious behavioural modifications. This confirms that the electrophysiological modifications started within the basal ganglia and could be transmitted to the cortex, leading to behavioural changes. Apart from the recent description of the caudate nucleus generating epileptic activity during stereoelectroencephalographic recordings in humans (Aupy et al. 2018), the acute disinhibition of the putamen has never been reported to generate motor seizures.

Worbe et al. showed that, if the firing frequency of the SPNs located near the bicuculline injection site increased, the firing frequency of the neurons located further away in the striatum decreased (Worbe et al. 2009). This suggests that local injections of bicuculline could change the entire dynamics of the striatal network, with a complex effect on the more distant neurons which are not directly influenced by the GABAergic antagonist. Although SPNs receive axonal collaterals from neighbouring SPNs (Kawaguchi 1993), their low intrinsic activity and the distal dendritic termination of collaterals on SPNs suggest that these interactions are probably weak. Thus, the main effect of bicuculline might be at the level of the somatic or dendritic terminations of the striatal GABAergic interneurons, particularly those of the fast-spiking type (FSIs) (Koos and Tepper 1999b; Koos 2004; Mallet et al. 2005). GABAergic interneurons are known to exert a powerful inhibition on the SPNs and to form extended networks throughout the entire striatum. It is likely that GABAergic antagonist mimics a decrease in the activity of these GABAergic interneurons, which could explain the changes observed outside the injection zone.

The fact that we observed a similar yet delayed paroxysmal LFP activity between the GPi and the putamen suggests that the putaminal oscillatory activity may propagate through the BG from the input to the output structure. However, the question of whether bicuculline-induced striatal activity modifications affect the direct or indirect striato-pallidal pathways (or

both) remains unresolved. In addition, as we did not have the opportunity to record the motor thalamus, we cannot verify whether these abnormal striato-pallidal oscillations propagate through it or not. Nevertheless, the delay between subcortical, cortical and muscular activity remains compatible with the propagation of motor activity through the corticospinal pathway (Ludolph et al. 1987).

How can we relate the dramatic electrophysiological changes observed within the sensorimotor striatum induced by bicuculline injection with the epileptic activity recorded from EEG? The sharp modulation of striatal inhibition after bicuculline injection could alter the level of synchrony within the striato-thalamo-cortical pathway. Indeed, the coherence between the cortex and the three basal ganglia nuclei increased dramatically in almost all the frequency bands during epileptic seizures compared to the background activity during saline control injections. This is concordant with the available data in monkeys (Darbin and Wichmann 2008) and humans, as shown by stereoelectroencephalographic recordings during focal seizures (Aupy et al. 2019). Sharott et al. showed that coordinated activity of fast spiking interneurons may be involved in mediating oscillatory synchronization within the striatum (Sharott et al. 2009). In addition, an abnormal striatal feedforward inhibition due to GABAergic fast spiking interneurons can promote synchronous oscillatory activity in the striato-thalamo-cortical network during absence seizures (Arakaki et al. 2016). This was corroborated in rodent GAERS experiments, as striatal output neurons stopped firing during spike-and-wave discharges, then displayed a rebound of activity (Slaght 2004). More recently, Miyamato et al. showed that pharmacological inhibition of cortico-striatal FSI excitatory transmission could trigger absences and convulsive seizures in mice (Miyamoto et al. 2019). Thus, it is likely that injecting GABAergic antagonist within the sensorimotor striatum could dramatically modify the synaptic excitatory/inhibitory balance of the basal ganglia output structure neurons (mainly the GPi in primate) and potentially alter cortical excitability, thereby triggering seizures.

In conclusion, we demonstrate that focal motor epileptic seizures can be induced by focal pharmacological manipulation of the basal ganglia in non-human primates. This reveals the strong impact of the sensorimotor striatum on cortical excitability. This does not mean that epileptic seizures might originate within the striatum but that this subcortical region could play a critical role in the pathophysiology of focal motor seizures through the regulation of cortical excitability. This striato-cortical pathway may not be part of seizure propagation pathways per se. Nevertheless, striatal acute desinhibition may lead to dramatic changes in the activity of this seizure "gating" pathways influencing seizure susceptibility by modulating the

threshold for the initiation and/or propagation of the seizures. Thus, modulation of striatal GABA levels may therefore represent a pharmacological target of interest in the treatment of seizures. Furthermore, a better understanding of the role of the basal ganglia during focal seizures would help in determining which type of epilepsy (epileptogenic zone or networks) might be most likely to benefit from deep brain stimulation.

AKNOLEDGMENT

The authors want to thank Hugues Orignac and François Georges for their precious help.

FUNDING

J.A. was supported by the Fondation pour la Recherche Médicale (bourse médico-scientifique FRM: FDM20150632965) and Servier Institute (bourse de mobilité)

COMPETING INTERESTS

None reported

AUTHOR CONTRIBUTIONS

JA contributed to conception, design and draft of the work, acquisition, analysis, and interpretation of data. BR contributed to acquisition, analysis and interpretation of data. SD contributed to acquisition, analysis and interpretation of data. MD contributed to analysis of data and substantial revision of the draft. NB contributed to analysis of data, TN contributed to acquisition of data. DG and PB contributed to conception and design of the work and substantial revision of the draft.

REFERENCES

Albin RL, Young AB, Penney JB. 1989. The functional anatomy of basal ganglia disorders. Trends in Neurosciences. 12:366–375.

Arakaki T, Mahon S, Charpier S, Leblois A, Hansel D. 2016. The Role of Striatal Feedforward Inhibition in the Maintenance of Absence Seizures. J Neurosci. 36:9618–9632.

Aupy J, Kheder A, Bulacio J, Chauvel P, Gonzalez-Martinez J. 2018. Is the caudate nucleus capable of generating seizures? Evidence from direct intracerebral recordings. Clin Neurophysiol. 129:931–933.

Aupy J, Wendling F, Taylor K, Bulacio J, Gonzalez-Martinez J, Chauvel P. 2019. Cortico-striatal synchronization in human focal seizures. Brain. 18:63–14.

Bachiega JC, Blanco MM, Perez-Mendes P, Cinini SM, Covolan L, Mello LE. 2008. Behavioral characterization of pentylenetetrazol-induced seizures in the marmoset. Epilepsy & Behavior. 13:70–76.

Bolam JP, Hanley JJ, Booth PA, Bevan MD. 2000. Synaptic organisation of the basal ganglia. J Anat. 196 (Pt 4):527–542.

Bonini F, McGonigal A, Tr buchon AS, Gavaret M, Bartolomei F, Giusiano B, Chauvel P. 2013. Frontal lobe seizures: From clinical semiology to localization. Epilepsia. 55:264–277.

Buzsáki G, Anastassiou CA, Koch C. 2012. The origin of extracellular fields and currents — EEG, ECoG, LFP and spikes. Nat Rev Neurosci. 13:407–420.

Crossman AR, Mitchell IJ, Sambrook MA, Jackson A. 1988. Chorea and myoclonus in the monkey induced by gamma-aminobutyric acid antagonism in the lentiform complex. The site of drug action and a hypothesis for the neural mechanisms of chorea. Brain. 111 (Pt 5):1211–1233.

Darbin O, Wichmann T. 2008. Effects of striatal GABA A-receptor blockade on striatal and cortical activity in monkeys. J Neurophysiol. 99:1294–1305.

DeLong M, Wichmann T. 2010. Changing views of basal ganglia circuits and circuit disorders. Clin EEG Neurosci. 41:61–67.

DeLong MR, Wichmann T. 2007. Circuits and circuit disorders of the basal ganglia. Arch Neurol. 64:20–24.

Deransart C, Depaulis A. 2002. The control of seizures by the basal ganglia? A review of experimental data. Epileptic Disord. 4 Suppl 3:S61–S72.

Deransart C, Lê B-T, Marescaux C, Depaulis A. 1998. Role of the subthalamo-nigral input in the control of amygdala-kindled seizures in the rat. Brain Res. 807:78–83.

Deransart C, Riban V, Lê B, Marescaux C, Depaulis A. 2000. Dopamine in the striatum modulates seizures in a genetic model of absence epilepsy in the rat. NEUROSCIENCE. 100:335–344.

Devergnas A, Piallat B, Prabhu S, Torres N, Louis Benabid A, David O, Chabardès S. 2012. The subcortical hidden side of focal motor seizures: evidence from micro-recordings and local field potentials. Brain. 135:2263–2276.

Dybdal D, Gale K. 2000. Postural and anticonvulsant effects of inhibition of the rat subthalamic nucleus. Journal of Neuroscience. 20:6728–6733.

Frey S, Comeau R, Hynes B, Mackey S, Petrides M. 2004. Frameless stereotaxy in the nonhuman primate. NeuroImage. 23:1226–1234.

Gittis AH, Leventhal DK, Fensterheim BA, Pettibone JR, Berke JD, Kreitzer AC. 2011. Selective Inhibition of Striatal Fast-Spiking Interneurons Causes Dyskinesias. Journal of Neuroscience. 31:1–5.

Gittis AH, Nelson AB, Thwin MT, Palop JJ, Kreitzer AC. 2010. Distinct Roles of GABAergic Interneurons in the Regulation of Striatal Output Pathways. Journal of Neuroscience. 30:2223–2234.
Haber SN. 2016. Corticostriatal circuitry. Dialogues in clinical neuroscience. 1–15.
Kaniff TE, Chuman CM, Neafsey EJ. 1983. Substantia nigra single unit activity during penicillin-induced focal cortical epileptiform discharge in the rat. Brain Research Bulletin. 11:11–13.
Kawaguchi Y. 1993. Physiological, morphological, and histochemical characterization of three classes of interneurons in rat neostriatum. Journal of Neuroscience. 13:4908–4923.
Koos T. 2004. Comparison of IPSCs Evoked by Spiny and Fast-Spiking Neurons in the Neostriatum. Journal of Neuroscience. 24:7916–7922.
Koos T, Tepper JM. 1999a. Inhibitory control of neostriatal projection neurons by GABAergic interneurons. Nat Neurosci. 2:467–472.
Koos T, Tepper JM. 1999b. Inhibitory control of neostriatal projection neurons by GABAergic interneurons. Nat Neurosci. 2:467–472.
Lalla L, Orozco PER, Jurado-Parras M-T, Brovelli A, Robbe D. 2017. Local or Not Local: Investigating the Nature of Striatal Theta Oscillations in Behaving Rats. eNeuro. 4:ENEURO.0128–17.2017.
Ludolph AC, Hugon J, Spencer PS. 1987. Non-invasive assessment of the pyramidal tract and motor pathway of primates. Electroencephalography and Clinical Neurophysiology. 67:63–67.
Mallet N, Le Moine C, Charpier S, Gonon F. 2005. Feedforward inhibition of projection neurons by fast-spiking GABA interneurons in the rat striatum in vivo. J Neurosci. 25:3857–3869.
Marmor O, Valsky D, Joshua M, Bick AS, Arkadir D, Tamir I, Bergman H, Israel Z, Eitan R. 2017. Local vs. volume conductance activity of field potentials in the human subthalamic nucleus. J Neurophysiol. 117:2140–2151.
MARSDEN CD, MELDRUM BS, Pycock C, TARSY D. 1975. Focal myoclonus produced by injection of picrotoxin into the caudate nucleus of the rat. J Physiol (Lond). 246:96P–96P.
McCairn KW, Bronfeld M, Belelovsky K, Bar-Gad I. 2009. The neurophysiological correlates of motor tics following focal striatal disinhibition. Brain. 132:2125–2138.
Mitzdorf U. 1985. Current source-density method and application in cat cerebral cortex: investigation of evoked potentials and EEG phenomena. Physiological Reviews. 65:37–100.
Miyachi S, Lu X, Imanishi M, Sawada K, Nambu A, Takada M. 2006. Somatotopically arranged inputs from putamen and subthalamic nucleus to primary motor cortex. Neuroscience Research. 56:300–308.
Miyamoto H, Tatsukawa T, Shimohata A, Yamagata T, Suzuki T, Amano K, Mazaki E, Raveau M, Ogiwara I, Oba-Asaka A, Hensch TK, Itohara S, Sakimura K, Kobayashi K, Kobayashi K, Yamakawa K. 2019. Impaired cortico-striatal excitatory transmission triggers epilepsy. Nature Communications. 1–13.
Nambu A. 2011. Somatotopic organization of the primate Basal Ganglia. Front Neuroanat. 5:26.
Neafsey EJ, Chuman CM, Ward AA. 1979. Propagation of focal cortical epileptiform discharge to the basal ganglia. Experimental Neurology. 66:97–108.
Norden AD, Blumenfeld H. 2002. The role of subcortical structures in human epilepsy. Epilepsy & Behavior. 3:1–13.
Paz JT, Deniau J-M, Charpier S. 2005. Rhythmic bursting in the cortico-subthalamo-pallidal network during spontaneous genetically determined spike and wave discharges. J

Neurosci. 25:2092–2101.
Paz JT, Huguenard JR. 2015. Microcircuits and their interactions in epilepsy: is the focus out of focus? Nat Neurosci. 18:351–359.
Perez-Mendes P, Blanco MM, Calcagnotto ME, Cinini SM, Bachiega J, Papoti D, Covolan L, Tannus A, Mello LE. 2011. Modeling epileptogenesis and temporal lobe epilepsy in a non-human primate. Epilepsy Research. 96:45–57.
Racine RJ. 1972. Modification of seizure activity by electrical stimulation. II. Motor seizure. Electroencephalography and Clinical Neurophysiology. 32:281–294.
Sharott A, Moll CKE, Engler G, Denker M, Grun S, Engel AK. 2009. Different Subtypes of Striatal Neurons Are Selectively Modulated by Cortical Oscillations. Journal of Neuroscience. 29:4571–4585.
Slaght SJ. 2004. On the Activity of the Corticostriatal Networks during Spike-and-Wave Discharges in a Genetic Model of Absence Epilepsy. Journal of Neuroscience. 24:6816–6825.
Szabo J, Cowan WM. 1984. A stereotaxic atlas of the brain of the cynomolgus monkey (Macaca fascicularis). J Comp Neurol. 222:265–300.
TARSY D, PYCOCK CJ, MELDRUM BS, MARSDEN CD. 2005. FOCAL CONTRALATERAL MYOCLONUS PRODUCED BY INHIBITION OF GABA ACTION IN THE CAUDATE NUCLEUS OF RATS. Brain. 101:1–20.
Vuong J, Devergnas A. 2017. The role of the basal ganglia in the control of seizure. Journal of Neural Transmission. 125:1–15.
Westerink BH, De Vries JB. 2001. A method to evaluate the diffusion rate of drugs from a microdialysis probe through brain tissue. Journal of Neuroscience Methods. 109:53–58.
Wong RK, Miles R, Traub RD. 1984. Local circuit interactions in synchronization of cortical neurones. Journal of Experimental Biology. 112:169–178.
Worbe Y, Baup N, Grabli D, Chaigneau M, Mounayar SP, McCairn K, F ger J, Tremblay LO. 2009. Behavioral and Movement Disorders Induced by Local Inhibitory Dysfunction in Primate Striatum. Cerebral Cortex. 19:1–13.
Yoshida M, Nagatsuka Y, Muramatsu S, Niijima K. 1991. Differential roles of the caudate nucleus and putamen in motor behavior of the cat as investigated by local injection of GABA antagonists. Neuroscience Research. 10:34–51.

FIGURE LEGENDS

Figure 1: histological reconstruction and immunohistological diffusion analysis

Histological reconstruction confirmed that neuronavigation and stereotactic implantations of the cannula and the linear micro-electrode array (LMA) targeted respectively the sensorimotor part of the putamen, posterior to the anterior commissure and the GPi tip allowing the recording of the entire lenticular nucleus (A). 3-D immunohistological studies in rats (B) and non-human primate (C) showed that the volume of diffusion of CTB remained confined within the putamen, without cortical diffusion.

Figure 2: Racines's scale averaged values and classical evolution during bicuculline injections

(A) A total of 39 bicuculline injections were performed and produced reproducible and dramatic behavioural changes, as confirmed by the averaged Racine's scale for each monkey compared to NaCl injections.

(B) Example of classical temporal evolution of behavioural changes during bicuculline injections showing the onset of myoclonia in the first 10 minutes, not stopping until injection of benzodiazepine.

Figure 3: Cortical and subcortical electrophysiological modifications during myoclonia and tonic-clonic seizures.

(A) Electromyographic activity recorded from extensor carpis radialis contralateral to injection site (sampling 1 KHz, band-pass filter between 1 and 70 Hz). T0 corresponds to onset of generalized tonic-clonic seizure (full line), while each preceding EMG burst corresponds to myoclonia (dash line).

(B) EEG activity recorded from electrodes above primary motor cortex ipsilateral to injection site (bipolar montage, sampling 1 KHz, band-pass filter between 1 and 70 Hz). Each EMG myoclonic burst is concomitant with paroxysmal activity characterized by a spike-and-wave followed by polyspikes. Generalized tonic-clonic seizure begins with the same paroxysmal pattern, followed by rhythmic spiking activity within the alpha band. Spiking activity tends to increase in amplitude (neuronal recruitment), while the inter-spike interval tends to increase until the end of seizure characterized by an abrupt offset.

(C) Close-up view of seizure onset (5 s before and after T0) with time-frequency analysis. TFA allows the analysis of the temporospectral content of EEG signals with a good resolution

in both time and frequency and assesses the clear-cut increase in frequency within the primary motor cortex region during myoclonia and seizure.

(D) Subcortical local field potential activity within the putamen, the GPe and the GPi (bipolar montage, sampling 1 KHz, band-pass filter between 1 and 70 Hz), respectively. Myoclonia and seizure are characterized by paroxysmal activity similar to that in cortex within the three-recorded subcortical regions, suggesting that epileptic activity could be recorded in the basal ganglia.

Figure 4: Results of spikes, backaveraging and coherence analysis.

(A) Automatic spike-and-waves detection showing a clear increase in the number of spikes-and-waves between Generalized tonic-clonic (GTC) seizures and sham (NaCl) injections ($p < 0.0001$, Student's t-test), myoclonic seizures and sham injections ($p < 0.0001$) and between GTC and myoclonic seizures ($p < 0.0001$).

(B) Back-averaging of hundreds of myoclonia episodes, revealing the emergence of a "retro" evoked potential within the cortex and the subcortical regions preceding the onset of myoclonia. The horizontal dashed lines correspond to the averaged and normalized electrophysiological signal (EEG and LFP) and its standard deviations (2 SD). Vertical dashed lines correspond to the beginning of the evoked potential (i.e. the moment when the first derivative of the signal fate exceeds two standard deviations for a duration of at least 25 ms). The vertical full line corresponds to the onset of the EMG myoclonia. Back-averaging analysis confirms that the first electrophysiological modifications appeared within the subcortical regions (putamen and GPe, followed by GPi) before the cortical electrophysiological changes and the occurrence of myoclonia.

(C) Averaged values of back-averaging (4.737 myoclonia analysed). Student t-test **** = $p < 0.0001$, *** = $p < 0.001$, ** = $p < 0.01$.

(D) In comparison with background activity (after saline injections), cortico-subcortical functional coupling during GTC seizures showed a significant increase in putamen/cortex, GPe/cortex and GPi/cortex magnitude-squared coherence within all the frequency bands ($p < 0.0001$, Student t-test).

Table 1: Behavioural effect of the Bicuculline injection and anatomical localization of the induced myoclonic jerks. N/A = not applicable; GTC = Generalized tonic clonic seizure

Animal	Injection n°	Volume (µL)	Onset (min)	Myoclonia anatomical distribution
Ra	1	4	16.5	Orofacial ± forelimbs and hind limbs
	2	4	17.5	Orofacial ± forelimbs
	3	2	20	Orofacial ± forelimbs
	4	2	17	Orofacial ± forelimbs
	5	2	N/A	No effect
	6	2	20	Orofacial ± forelimbs ± hind limbs ± bilatéralisation and GTC
	7	1	21.5	Orofacial ± forelimbs ± hind limbs
	8	1	22	Orofacial ± forelimbs
	9	0.5	19.5	Orofacial
	10	0.5	29	Orofacial ± forelimbs
	11	0.5	N/A	No effect
	12	4	15	Orofacial ± forelimbs ± hind limbs
	13	2	N/A	No effect
	14	4	14	Orofacial ± forelimbs
	15	4	N/A	No effect
	16	4	18	Orofacial ± forelimbs
Average (SD)		2.8 (1.2)	19.4 (4.7)	
Ze	1	2	13	Forelimbs ± orofacial ± hind limbs ± bilateralisation and GTC
	2	2	8	Forelimbs ± orofacial ± hind limbs ± bilateralisation and GTC
	3	2	11.5	Forelimbs ± orofacial
	4	1	10	Forelimbs ± orofacial
	5	1	8.5	Forelimbs ± orofacial
	6	2	8	Forelimbs ± orofacial ± hind limbs ± bilateralisation and GTC
	7	2	N/A	No effect
	8	2	N/A	No effect
	9	2	40	Forelimbs
	10	2	60	Forelimbs ± orofacial ± hind limbs ± bilateralisation and GTC
	11	2	N/A	No effect
	12	2	N/A	No effect
Average (SD)		1.8 (0.4)	23.2 (21.8)	
Di	1	4	N/A	No effect
	2	4	4	Forelimbs
	3	4	1.5	Forelimbs
	4	4	N/A	No effect
	5	4	1.5	Forelimbs ± orofacial ± hind limbs ± bilateralisation and GTC
	6	4	3	Forelimbs
	7	4	2	Forelimbs
	8	2	7.5	Forelimbs ± orofacial ± hind limbs ± bilateralisation and GTC
	9	4	10.5	Forelimbs ± orofacial
	10	4	12.5	Forelimbs ± orofacial ± hind limbs ± bilateralisation and GTC
	11	2	N/A	No effect
Average (SD)		3.6 (0.8)	3.0 (1.0)	

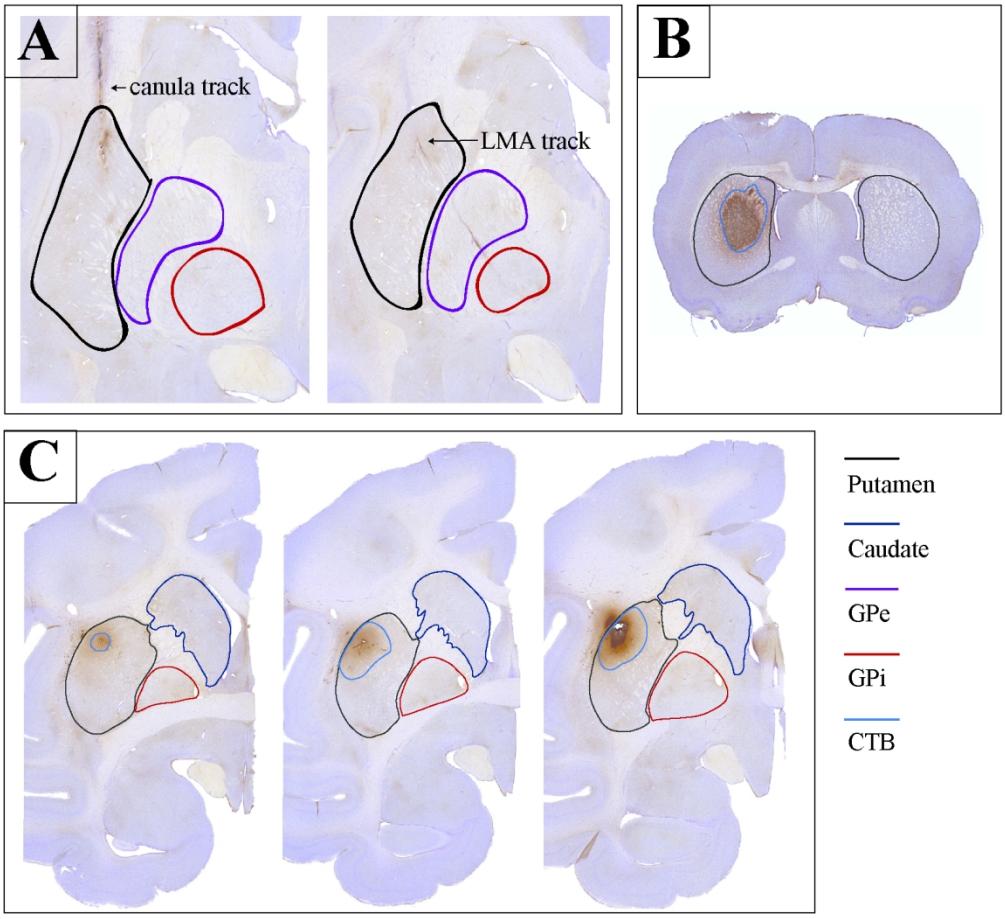

Figure 1: histological reconstruction and immunohistological diffusion analysis
Histological reconstruction confirmed that neuronavigation and stereotactic implantations of the cannula and the linear micro-electrode array (LMA) targeted respectively the sensorimotor part of the putamen, posterior to the anterior commissure and the GPi tip allowing the recording of the entire lenticular nucleus (A). 3-D immunohistological studies in rats (B) and non-human primate (C) showed that the volume of diffusion of CTB remained confined within the putamen, without cortical diffusion.

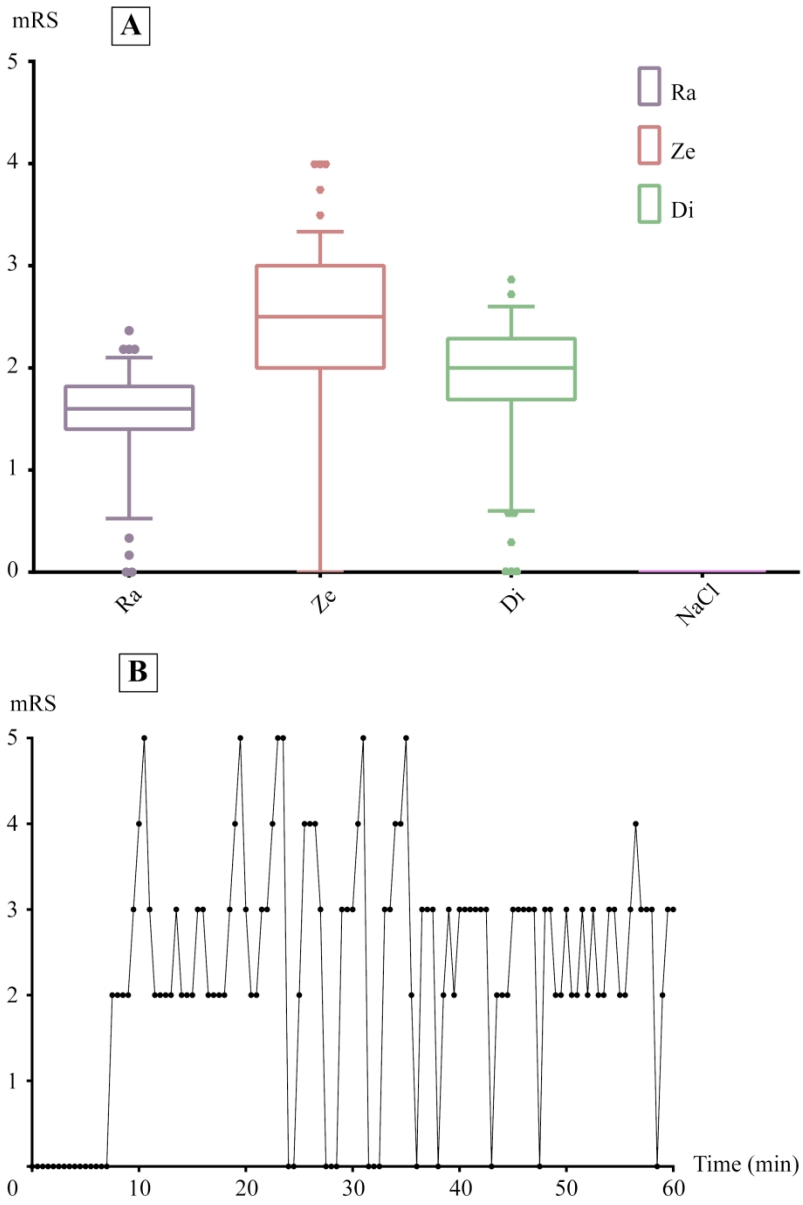

Figure 2: Racines's scale averaged values and classical evolution during bicuculline injections
(A) A total of 39 bicuculline injections were performed and produced reproducible and dramatic behavioural changes, as confirmed by the averaged Racine's scale for each monkey compared to NaCl injections.
(B) Example of classical temporal evolution of behavioural changes during bicuculline injections showing the onset of myoclonia in the first 10 minutes, not stopping until injection of benzodiazepine.

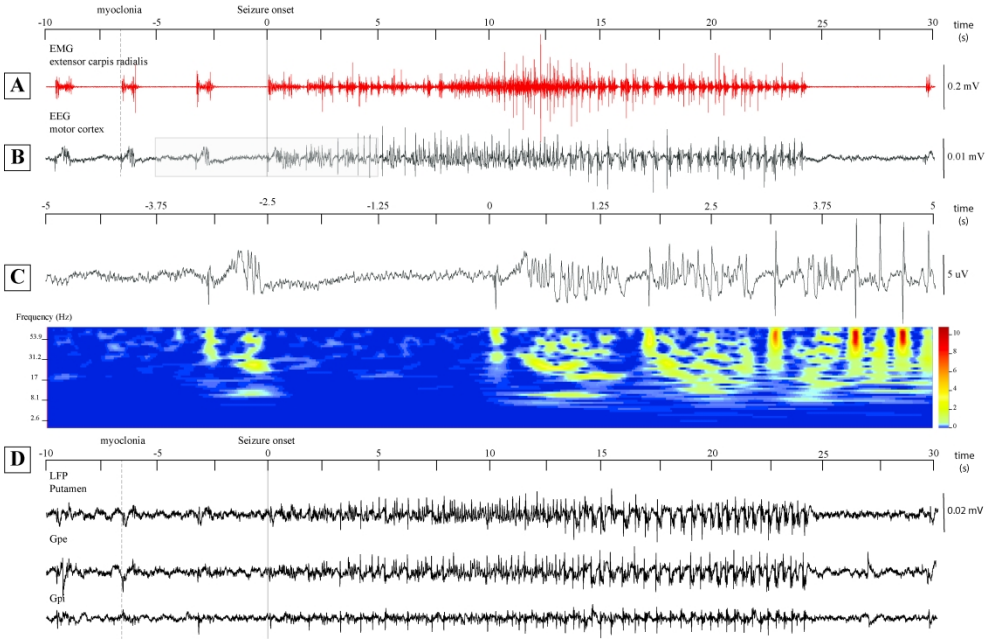

Figure 3: Cortical and subcortical electrophysiological modifications during myoclonia and tonic-clonic seizures.

(A) Electromyographic activity recorded from extensor carpis radialis contralateral to injection site (sampling 1 KHz, band-pass filter between 1 and 70 Hz). T0 corresponds to onset of generalized tonic-clonic seizure (full line), while each preceding EMG burst corresponds to myoclonia (dash line).

(B) EEG activity recorded from electrodes above primary motor cortex ipsilateral to injection site (bipolar montage, sampling 1 KHz, band-pass filter between 1 and 70 Hz). Each EMG myoclonic burst is concomitant with paroxysmal activity characterized by a spike-and-wave followed by polyspikes. Generalized tonic-clonic seizure begins with the same paroxysmal pattern, followed by rhythmic spiking activity within the alpha band. Spiking activity tends to increase in amplitude (neuronal recruitment), while the inter-spike interval tends to increase until the end of seizure characterized by an abrupt offset.

(C) Close-up view of seizure onset (5 s before and after T0) with time-frequency analysis. TFA allows the analysis of the temporospectral content of EEG signals with a good resolution in both time and frequency and assesses the clear-cut increase in frequency within the primary motor cortex region during myoclonia and seizure.

(D) Subcortical local field potential activity within the putamen, the GPe and the GPi (bipolar montage, sampling 1 KHz, band-pass filter between 1 and 70 Hz), respectively. Myoclonia and seizure are characterized by paroxysmal activity similar to that in cortex within the three-recorded subcortical regions, suggesting that epileptic activity could be recorded in the basal ganglia.

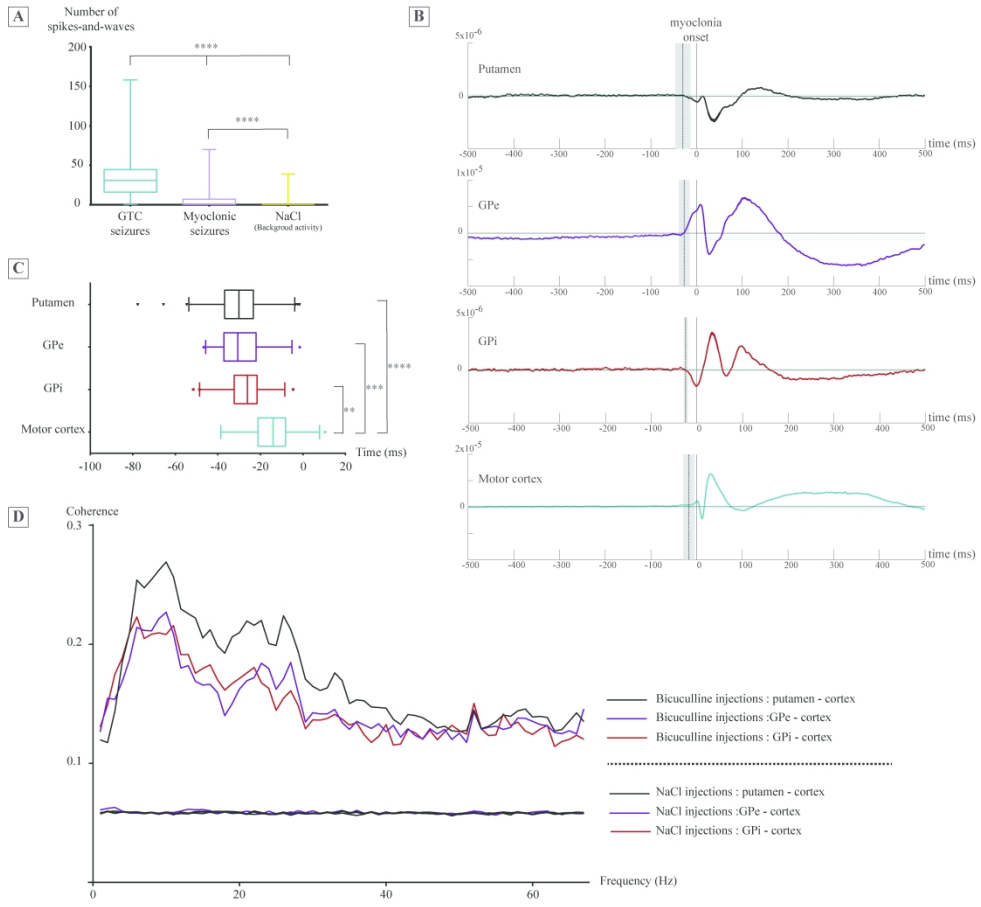

Figure 4: Results of spikes, backaveraging and coherence analysis.
(A) Automatic spike-and-waves detection showing a clear increase in the number of spikes-and-waves between Generalized tonic-clonic (GTC) seizures and sham (NaCl) injections ($p < 0.0001$, Student's t-test), myoclonic seizures and sham injections ($p < 0.0001$) and between GTC and myoclonic seizures ($p < 0.0001$).
(B) Back-averaging of hundreds of myoclonia episodes, revealing the emergence of a "retro" evoked potential within the cortex and the subcortical regions preceding the onset of myoclonia. The horizontal dashed lines correspond to the averaged and normalized electrophysiological signal (EEG and LFP) and its standard deviations (2 SD). Vertical dashed lines correspond to the beginning of the evoked potential (i.e. the moment when the first derivative of the signal fate exceeds two standard deviations for a duration of at least 25 ms). The vertical full line corresponds to the onset of the EMG myoclonia. Back-averaging analysis confirms that the first electrophysiological modifications appeared within the subcortical regions (putamen and GPe, followed by GPi) before the cortical electrophysiological changes and the occurrence of myoclonia.
(C) Averaged values of back-averaging (4.737 myoclonia analysed). Student t-test **** = $p < 0.0001$, *** = $p < 0.001$, ** = $p < 0.01$.
(D) In comparison with background activity (after saline injections), cortico-subcortical functional coupling during GTC seizures showed a significant increase in putamen/cortex, GPe/cortex and GPi/cortex magnitude-squared coherence within all the frequency bands ($p < 0.0001$, Student t-test).

Acute and focal striatal disinhibition induces motor epileptic seizures

Aupy J. MD PhD [1, 2] *, Ribot B. PhD [1] *, Dovero S PhD [1], Biendon N. [1], Nguyen T-H [1], Deffains M PhD [1], Guehl D MD PhD [1, 2], Burbaud P MD PhD [1, 2].

[1] University of Bordeaux, Bordeaux Neurocampus, IMN, UMR CNRS 5293, Bordeaux, France

[2] Bordeaux University Hospital, Department of Clinical Neurosciences, Bordeaux, France

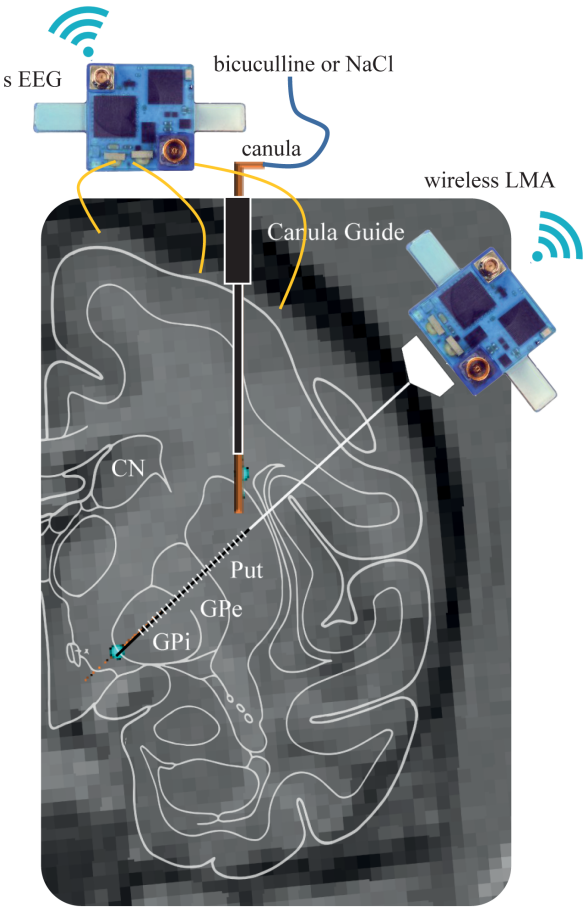

Supplemental data figure 1: Injections and recording procedure based on neuronavigation MRI and stereotactic atlas

The site of injections was determined on presurgical neuronavigation MRI and compared to a stereotactic atlas. The cannula guide targeted the sensorimotor striatum (tip position calculated to be 2 mm above the striatum, approximately 2.5 mm posterior to the anterior commissure and 12 mm lateral to the interhemispheric line). Cortical and subcortical (lenticular) activity was chronically and wirelessly recorded using EEG and linear microelectrode array (LMA) fixed in the monkey's skull. EEG pins and LMA position were determined on presurgical MRI and compared to a stereotactic atlas. The injection cannula connected via a Delrin manifold to a 10-ml syringe was inserted in the sensorimotor striatum (extending 2.5 to 4 mm beyond the cannula guide tip) and left in place throughout the experiment. Low volumes (0.5 to 4 µL) of bicuculline or sham NaCl were injected slowly at 1 µL/min. EEG = electroencephalogram, LMA = linear microelectrode array, CN = caudate nucleus, Put = putamen, GPe = Globus pallidus internus, GPi = globus pallidus internus.

Monkey	1	2		3	
	Cannula guide tip	Cannula guide tip	GPi tip	Cannula guide tip	GPi tip
Laterality	11	-13	-3.5	11.5	22.5
Anteriority	-2	-2.5	-2.5	-2.5	-3
Depth	-8	-6.5	4	-8.5	3.5

Supplemental table 1: Stereotactic coordinates of implanted cannulae and chronic linear multi array electrodes

Coordinates are reported to the anterior commissure (AC) in millimetres. For the first monkey no LMA electrodes had been implanted. For monkeys 2 and 3, both cannula and multicontact linear electrode had been implanted. A positive laterality corresponds to a shift to the right with respect to AC, a negative laterality indicates a shift to the left. A negative anteriority corresponds to a displacement behind AC.

	Rat 1	Rat 2	Monkey 3
Right putamen volume	41.3 mm^3	39.29 mm^3	484.86 mm^3
CTB volume	6.03 mm^3	6.99 mm^3	79.07 mm^3
% of the Putamen volume	14.6 %	17.8 %	16.3 %

Supplemental table 2: Results of the immunostaining against CTB

To estimate the volume of drugs diffusion, we performed an immunostaining raised against CTB on serial striatal sections of two rat brains and one monkey brain (monkey 3). These studies showed that the volume of diffusion of CTB was not bigger than 17.8 % of the entire putamen volume.

Supplemental Video 1: 3-D volume reconstruction of the immunostaining against CTB in rat

In red, 3-dimensional volume reconstruction of the immunostaining raised against CTB on serial striatal sections in rat in relation to the striatum (in green) and the cerebral cortex (in blue)

Supplemental Video 2: 3-D volume reconstruction of the immunostaining against CTB in monkey

In blue, 3-dimensional volume reconstruction of the immunostaining raised against CTB on serial striatal sections in rat in relation to the putamen (in green), the caudate nucleus (in turquoise) and the pallidum external (in green) and internal (in purple).

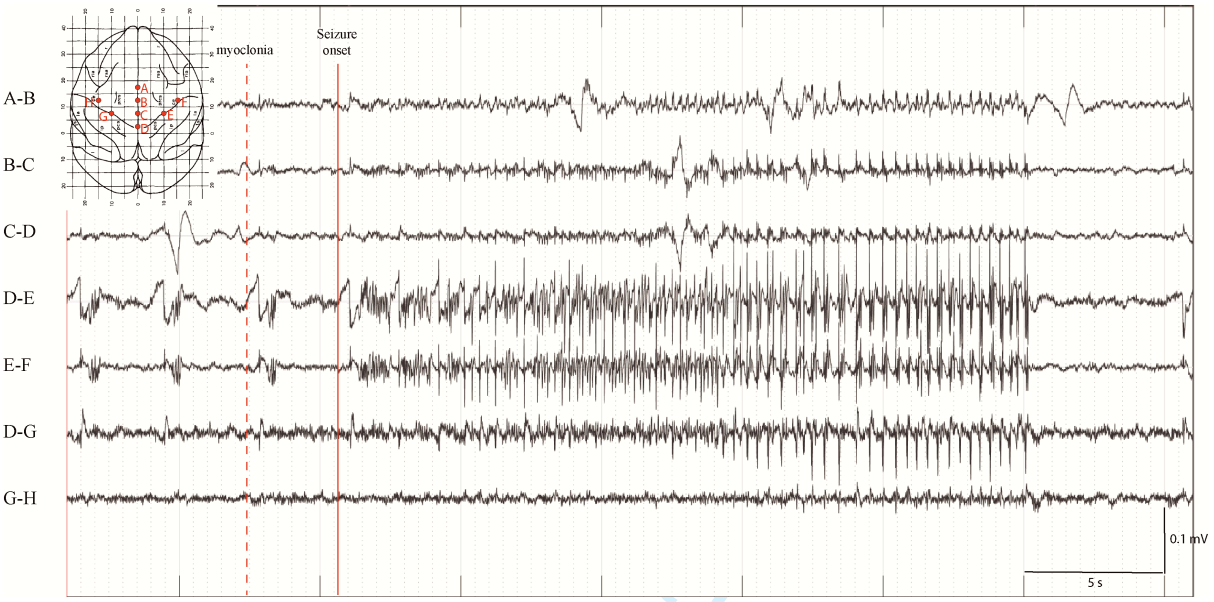

Supplemental figure 2: EEG recordings during myoclonic activity (red dash line) and generalized seizure (the red full line marking the onset). Bipolar recordings, band pass filter 0.5 – 70 Hz.

A-B correspond to the SMA region ; B-C to the premotor region ; C-D to the primary motor cortex region (posterior limbs) ; D-E and E-F to the left primary motor cortex region (anterior limbs, ipsilateral to the injection site) ; D-G and G-H to the right primary motor cortex region (anterior limbs, contralateral to the injection site). Myoclonia are characterized by a paroxysmal epileptic activity (spikes-and-waves followed by polyspkikes over the left primary motor cortex region (anterior limbs), ipsilateral to the injection site. Seizure starts with an abrupt onset with the same paroxysmal activity that tends to become rhythmical while the amplitude increase (neuronal recruitment). In addition, this electrophysiological epileptic activity will diffuse to the adjacent region ipsi and contralateral (generalized, bilateral, tonic-clonic seizure). Seizure will stop with an abrupt offset followed by global flattening.

Supplemental figure 3: LFP recordings during myoclonic activity (red dash line) and generalized seizure (the red full line marking the onset). Bipolar recordings over adjacent contacts, band pass filter 0.5 – 70 Hz.

At the subcortical level, myoclonia are characterized by a paroxysmal activity (spikes-and-waves followed by polyspkikes) over the entire lenticular nucleus. Seizure starts with an abrupt onset with the same paroxysmal activity that tends to become rhythmical while the amplitude increase (neuronal recruitment). Seizure will stop with an abrupt offset. It is interesting to note the multiple phase reversal between contiguous contacts in bipolar montage confirming that this electrophysiological activity is locally generated without far-field (cortical) contribution.